

AFLOW-CCE for the thermodynamics of ionic materials

Rico Friedrich^{1,2,3,*} and Stefano Curtarolo^{3,4,†}

¹Theoretical Chemistry, Technische Universität Dresden, 01062 Dresden, Germany

²Institute of Ion Beam Physics and Materials Research,
Helmholtz-Zentrum Dresden-Rossendorf, 01328 Dresden, Germany

³Center for Autonomous Materials Design, Duke University, Durham, NC 27708, USA

⁴Materials Science, Electrical Engineering, and Physics, Duke University, Durham, NC 27708, USA

(Dated: October 30, 2023)

Accurate thermodynamic stability predictions enable data-driven computational materials design. Standard density functional theory (DFT) approximations have limited accuracy with average errors of a few hundred meV/atom for ionic materials such as oxides and nitrides. Thus, insightful correction schemes as given by the coordination corrected enthalpies (CCE) method, based on an intuitive parameterization of DFT errors with respect to coordination numbers and cation oxidation states present a simple, yet accurate solution to enable materials stability assessments. Here, we illustrate the computational capabilities of our AFLOW-CCE software by utilizing our previous results for oxides and introducing new results for nitrides. The implementation reduces the deviations between theory and experiment to the order of the room temperature thermal energy scale, *i.e.* ~ 25 meV/atom. The automated corrections for both materials classes are freely available within the AFLOW ecosystem via the AFLOW-CCE module, requiring only structural inputs.

Keywords: formation enthalpies, data-driven research, computational materials science, high-throughput computing, ionic materials, AFLOW

In data-driven computational materials science, density functional theory (DFT) has become the standard method to characterize systems and an indispensable tool enabling insightful predictions. Over the last decades, John Perdew and his group have made DFT accurate enough for materials design while setting the standards in the field according to the functional developments related to LDA [1], PBE [2], and SCAN [3]. These approximations are used for the data generation of virtually all big materials databases with millions of entries [4–13], and thus closely match the quest posed by Dirac for “approximate practical methods” to solve the quantum many-body solid state problem [14].

Thermodynamics is one of the most crucial aspects for materials design, since synthesizability can be ensured for thermodynamically stable systems. As such, the need for an accurate computational treatment of thermodynamic stability is pressing for many issues related to *e.g.* stability of competing phases [15], high-entropy materials [16, 17], solution enthalpies in liquid metals [18], and novel (2D) nanostructures when evaluating relative energies and with respect to the bulk parent compound [19–23]. The formation enthalpy rigorously quantifies the thermodynamic stability, as the enthalpy difference between the material and its elemental references. Its accurate calculation is a basic challenge. Standard (semi-)local and even currently available more advanced *ab initio* methods yield errors of several hundred meV/atom for ionic compounds such as oxides and nitrides [24–32] when comparing to validated standard collections for thermochemical data [33–36]. The reason is that accurate total energies for all systems involved — compound and elemental references — are still not accessible with the standard functionals,

and errors when calculating the enthalpy difference between chemically dissimilar systems do not cancel. The explicit treatment of self-interaction errors might be an avenue to further significant advances from *ab initio* [37–40], but likely at an elevated computational cost infeasible for high-throughput materials design. Even efforts based on Quantum Monte Carlo calculations only partially remedy the discrepancies between theory and experiment [41–43].

A solution for this dilemma can be provided by physically motivated empirical enthalpy corrections. These parameterize (semi-)local DFT errors with respect to measured values, are hence feasible to enable materials design, and can include uncertainty quantification [44]. It turns out that correction methods, mixing schemes, and machine learning approaches based on only the composition of a material can already lead to significant improvements in accuracy reducing the mean absolute errors (MAEs) down to ~ 50 meV/atom [24–27, 45–48]. In addition to the still limited accuracy, such an approach can, however, be problematic for the phase diagrams of certain systems due to only tilting the Gibbs energy landscape [32]. These schemes do also not allow for a correction of the *relative* stability of polymorphs whose energetic ordering is known to be incorrectly predicted by DFT in several cases [30].

To rectify these issues, we have recently introduced the method of coordination corrected enthalpies (CCE), based on the bonding topology in a material [32]. CCE avoids thermodynamic paradoxes by construction, reduces the MAE down to ~ 25 meV/atom, and can correct the relative stability of polymorphs if they differ in the number of nearest neighbor bonds [32, 49]. So far, the method has been parameterized for oxides and a few halides calling for an extension to other anion classes such as nitrides. Most importantly, effective implementations are needed freely available to and easy to use by the computational materials science community. Here, we provide such a

* rico.friedrich@tu-dresden.de

† stefano@duke.edu

tool by our automated corrections within the AFLOW-CCE module.

In this article, we **i.** present some theoretical basics, a motivation of CCE, and its formalism; and **ii.** demonstrate the computational capabilities of our implementation using our previous results for oxides and new results for nitrides, including a discussion of the error bars of plain DFT for different standard functionals, as well as a demonstration of the performance of the AFLOW-CCE module for a test set of ternary nitrides.

THEORY

Formation enthalpies. From DFT, one directly computes an estimate of the formation enthalpy $\Delta_f E_{A_{x_1}B_{x_2}\dots Y_{x_n}}^{0,\text{DFT}}$ of a compound $A_{x_1}B_{x_2}\dots Y_{x_n}$ at zero temperature and pressure without zero-point vibrations:

$$\Delta_f E_{A_{x_1}\dots Y_{x_n}}^{0,\text{DFT}} = U_{A_{x_1}\dots Y_{x_n}}^{0,\text{DFT}} - \left[\sum_{i=1}^{n-1} x_i U_i^{0,\text{DFT}} + \frac{x_n}{2} U_{Y_2}^{0,\text{DFT}} \right],$$

where $U_{A_{x_1}\dots Y_{x_n}}^{0,\text{DFT}}$, $U_i^{0,\text{DFT}}$, and $U_{Y_2}^{0,\text{DFT}}$ are the total internal energies of the compound, the i -element reference phase, and molecular Y_2 , respectively; and x_1, \dots, x_n are stoichiometries. In this manuscript, Y stands for O or N and this notation can be extended to other anion species.

On the other hand, the tabulated measured standard (“o”) formation enthalpy at room temperature ($T_r = 298.15$ K) corresponds to:

$$\Delta_f H_{A_{x_1}\dots Y_{x_n}}^{\circ, T_r, \text{exp}} = H_{A_{x_1}\dots Y_{x_n}}^{\circ, T_r} - \left[\sum_{i=1}^{n-1} x_i H_i^{\circ, T_r} + \frac{x_n}{2} H_{Y_2}^{\circ, T_r} \right],$$

where $H_{A_{x_1}\dots Y_{x_n}}^{\circ, T_r}$, H_i°, T_r} , and $H_{Y_2}^{\circ, T_r}$ are the standard enthalpies of the compound, the i -element reference phase, and Y_2 at T_r .

As we have shown in Ref. 32, the measured value can be written in a very good approximation (accuracy better than 1 meV/atom) as the sum of the internal energy contribution and a small vibrational term $\Delta_f H_{A_{x_1}\dots Y_{x_n}}^{\text{vib}}$ of the order of 10-20 meV/atom due to zero-point and thermal effects:

$$\Delta_f H_{A_{x_1}\dots Y_{x_n}}^{\circ, T_r, \text{exp}} \approx \Delta_f E_{A_{x_1}\dots Y_{x_n}}^0 + \Delta_f H_{A_{x_1}\dots Y_{x_n}}^{\text{vib}} \approx \Delta_f H_{A_{x_1}\dots Y_{x_n}}^{\circ, T_r, \text{cal}}. \quad (1)$$

Both contributions in Eqn. (1) can be estimated computationally to yield $\Delta_f H_{A_{x_1}\dots Y_{x_n}}^{\circ, T_r, \text{cal}}$, the calculated standard formation enthalpy at T_r [32].

The vibrational term can be computed reliably within a quasi-harmonic Debye model as implemented within the AFLOW Automatic GIBBS Library (AGL) [50–55] with an average error as small as ~ 5 meV/atom [32]. The zero-point and thermal effects of O_2/N_2 are accounted for

based on reliable tabulated (spectroscopic) data [34] as well as assuming perfect gas behavior.

The large errors between calculated and measured formation enthalpies are due to estimating the internal energy contribution in Eqn. (1) from DFT.

Motivation of corrections per bond. To obtain accurate enthalpies, an insightful correction scheme is required. The idea behind CCE is illustrated in Fig. 1. When forming perovskite CaTiO_3 out of CaO and rutile TiO_2 , the number of nearest neighbor cation-anion bonds, *i.e.* the coordination number of Ca, changes from six to eight. The number of bonds in a material is crucial for its thermodynamic stability and it is commonly discussed how well a specific approximation to DFT captures a certain type of bonding [56]. It thus seems plausible to assign an error per bond to the computed enthalpies making the coordination number an appropriate descriptor to parameterize DFT errors. For optimal transferability from fit to target compounds, the correction also needs to be specific to the oxidation number of the cation as a different self-interaction error is expected for different charge states of transition metal centers such as Fe^{2+} *vs.* Fe^{3+} .

The CCE formalism. Taking binary compounds $A_{x_1}Y_{x_2}$ as the fit set, the CCE corrections $\delta H_{A-Y}^{T, A+\alpha}$ per cation-anion $A-Y$ bond and cation oxidation state $+\alpha$ are obtained from the difference between DFT formation enthalpies and experimental standard formation enthalpies at temperature T [32]:

$$\Delta_f E_{A_{x_1}Y_{x_2}}^{0,\text{DFT}} - \Delta_f H_{A_{x_1}Y_{x_2}}^{\circ, T, \text{exp}} = x_1 N_{A-Y} \delta H_{A-Y}^{T, A+\alpha},$$

where N_{A-Y} is the number of nearest neighbor $A-Y$ bonds and x_i are stoichiometries for the i -species. T can be 298.15 or 0 K, *i.e.* temperature effects are included in the corrections as 0 K estimates of experimental $\Delta_f H$ values can be obtained by taking into account thermal effects only for the fit compounds according to Ref. [49]. As detailed in Refs. [32, 49], the corrections are fit to the formation enthalpies directly calculated from DFT, without taking into account thermal/vibrational contributions since these terms are to a very good approximation (average accuracy ~ 1 meV/atom) implicitly included in the corrections.

The corrections can then be applied without additional computational cost compared to plain DFT to any multi-ary compound $A_{x_1}B_{x_2}\dots Y_{x_n}$ to obtain the CCE formation enthalpy $\Delta_f H_{A_{x_1}B_{x_2}\dots Y_{x_n}}^{\circ, T, \text{CCE}}$:

$$\Delta_f H_{A_{x_1}B_{x_2}\dots Y_{x_n}}^{\circ, T, \text{CCE}} = \Delta_f E_{A_{x_1}B_{x_2}\dots Y_{x_n}}^{0,\text{DFT}} - \sum_{i=1}^{n-1} x_i N_{i-Y} \delta H_{i-Y}^{T, i+\alpha},$$

where N_{i-Y} is the number of nearest neighbor bonds between the cation i and anion Y -species. The method has been implemented for automated enthalpy corrections requiring only an input structure as the AFLOW-CCE module available to the scientific community [49]. The implementation is also applicable to enthalpies computed

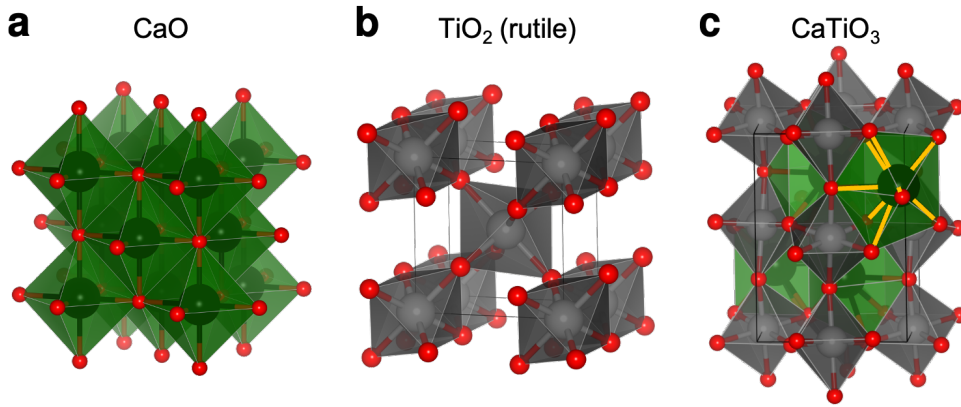


FIG. 1. **Corrections per bond.** Structural models of (a) CaO, (b) rutile TiO₂, and (c) perovskite CaTiO₃. While the Ti coordination number is six in both rutile and perovskite, Ca exhibits a coordination change from sixfold to eightfold when going from CaO to CaTiO₃ (Ca–O bonds marked in yellow). The number of bonds is thus a crucial parameter for the thermodynamic stability of a material.

from DFT+*U* if the same settings as for the AFLOW-ICSD database are used [49, 57].

The *ab-initio* calculations of this study for the exchange-correlation functionals LDA [1, 58, 59], PBE [2], and SCAN [3] are performed with AFLOW [4, 5, 60–65] and the Vienna *Ab-initio* Simulation Package (VASP) [66] with settings according to Refs. 32 and 57.

RESULTS AND DISCUSSION

Implementation: corrections for oxides. We first demonstrate the capabilities of our AFLOW-CCE implementation on our previous data for oxides included in the Supporting Information of Ref. 32. While absolute formation enthalpies are on the order of several eV/atom, Fig. 2 depicts the difference between computed (DFT+AGL) and measured room temperature formation enthalpies for 79 binary (a) and 71 ternary (b) oxides also including a visualization of the vibrational contribution in the lower panel in both cases. The errors for all functionals are substantial with SCAN delivering the most accurate results still showing overall MAEs of at least about 100 meV/atom. The MAEs over the whole binary set are 235, 176, and 105 meV/atom for PBE, LDA, and SCAN, respectively.

In general, PBE underestimates the (absolute) formation enthalpies meaning that they are less negative than the experimental values while LDA and SCAN mostly overestimate them. For the binaries, the *l*-character of the cation has, however, a strong influence. While SCAN yields constantly very accurate enthalpies with a MAE as small as 27 meV/atom for *s*-element oxides, all functionals show a systematic decrease of the computed values for heavier *p*-oxides which can be related to increasing covalency [32]. For the *d*-oxides, the systematic trends of the functionals are diminished and large individual errors ranging up to ~ 800 meV/atom are observed increasing also the MAEs to over 150 meV/atom. This drastic behavior for the rock salt structure *d*-oxides VO, MnO, FeO,

CoO, and NiO is well known [27, 32]. For the ternaries, mostly including transition metal elements, the large errors are confirmed with MAEs of at least 100 meV/atom for each functional.

The vibrational contribution is very small in all cases reaching at max about 20 meV/atom for Al₂O₃ and kyanite Al₂SiO₅ and as such are about two orders of magnitude smaller than absolute formation enthalpies.

The results from the binaries are then used to obtain the CCE corrections and to apply them to the ternary test set. Fig. 3 shows the example of the corrected SCAN results where we also compare to an implementation of the FERE method for our dataset (quasi-FERE). Both methods significantly decrease the plain DFT errors by a factor of 2 to 4 with the CCE MAE of 27 meV/atom being about half of the quasi-FERE one of 44 meV/atom. The latter accuracy agrees well with the previously reported MAEs of about 50 meV/atom of the other correction schemes [26, 27]. The CCE errorbar is thus on the order of room temperature thermal energy and may as such enable more exact thermodynamic stability predictions. CCE achieves the same accuracy for ternary halides [32]. Since it is based on the bonding topology in materials, the method can also correct the relative stability of different polymorphs as demonstrated for several systems and can yield accurate defect energies as exemplified for Ti-O Magnéli phases [32]. For a few systems with large errors after correction in Fig. 3 for both methods (CCE and quasi-FERE) such as FeAl₂O₄, the experimental values might be inaccurate and should potentially be revised.

Implementation: corrections for nitrides. The study of a suitable set of binary materials will first allow uncovering the errors of uncorrected DFT for this materials class, as well as deriving the corrections. The predictive power of the corrections will then be validated for ternary nitrides. The computed and corrected data of this part are included in the Appendix.

For an overview, in Fig. 4, elements forming binary nitrogen compounds with tabulated high quality thermo-

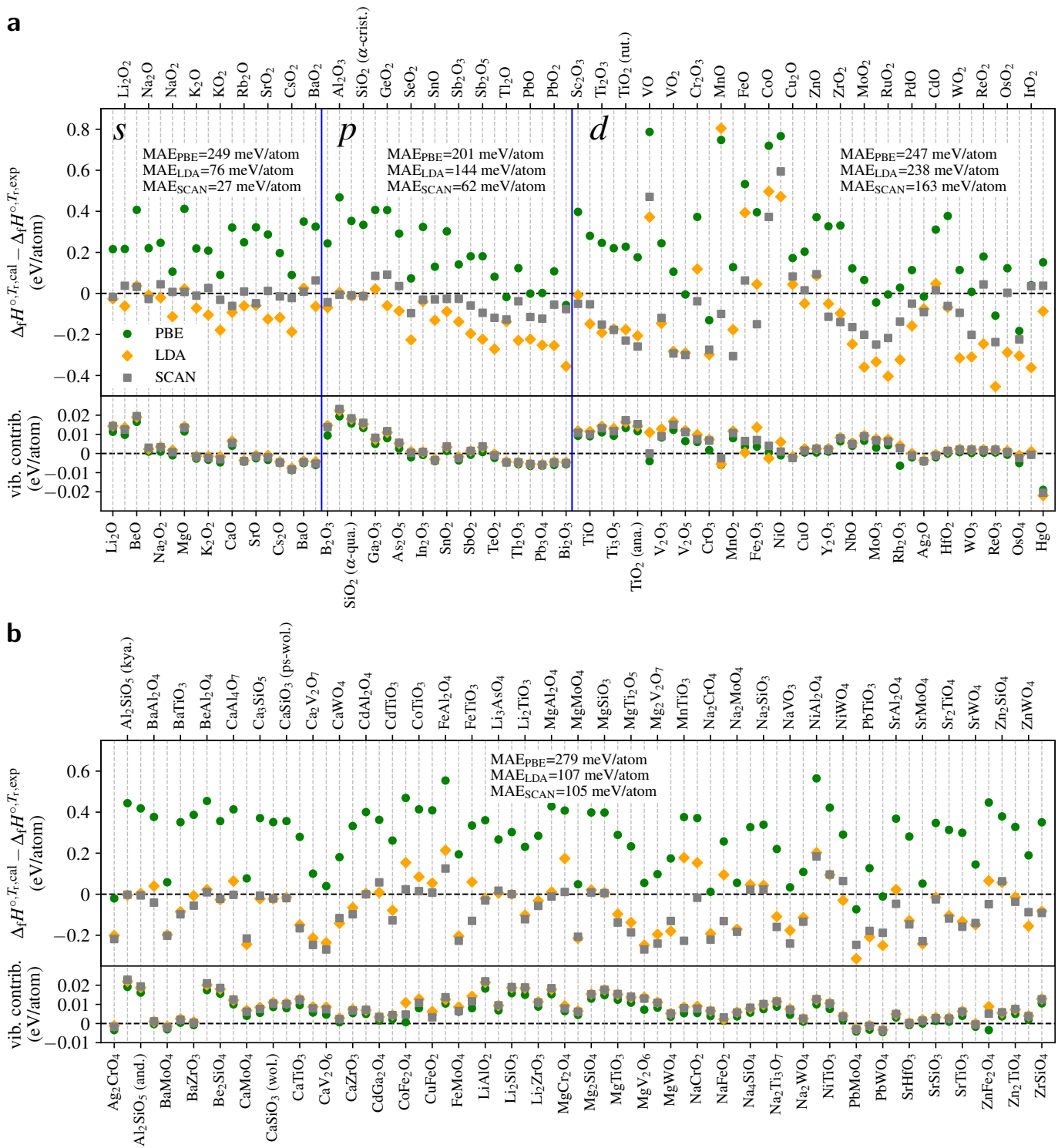


FIG. 2. **Formation enthalpies and vibrational contribution for binary oxides.** (a) Differences between calculated and experimental room temperature formation enthalpies of 79 binary oxides (upper panel) and vibrational (zero-point + thermal) contribution to the calculated formation enthalpy (lower panel) for three standard DFT functionals. Vertical blue lines separate blocks with different l -character of the cations. (b) Differences between calculated and experimental room temperature formation enthalpies of 71 ternary oxides (upper panel) and vibrational contribution (lower panel). Adapted from Ref. 32.

chemical data in the standard collections [33–36] are circled. Nitrides are much more scarce than oxides since there are only 20 binaries. The major reason is that the

N_2 molecular reference phase is thermodynamically exceptionally stable which makes it difficult to form a nitrogen compound with a net energy gain. Recent computa-

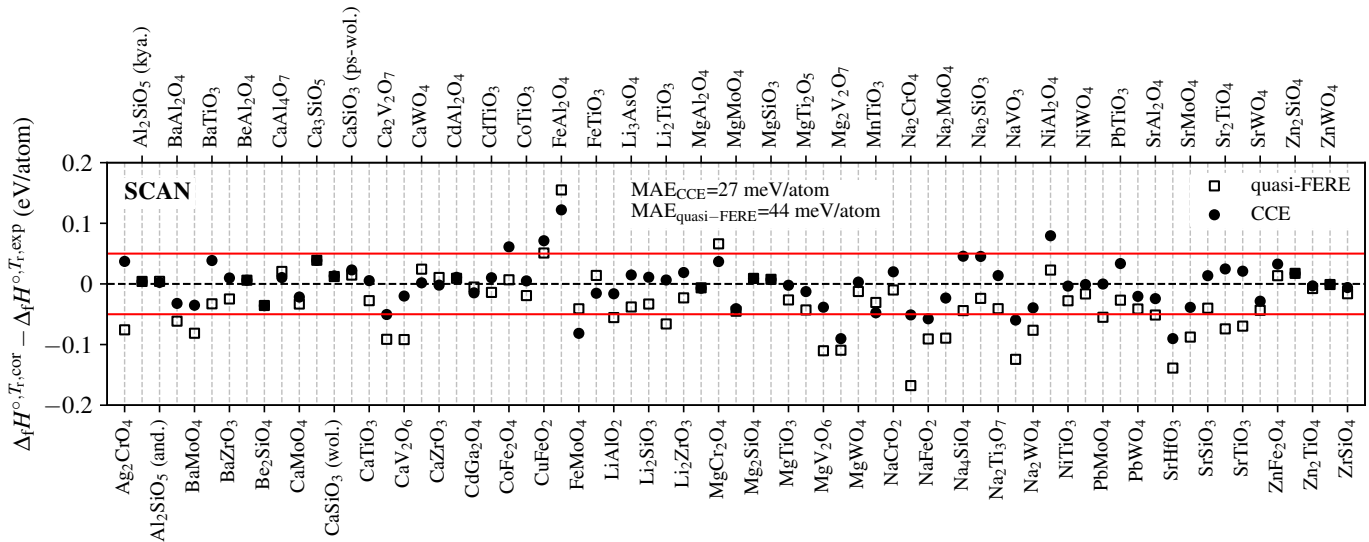


FIG. 3. **Corrected SCAN enthalpies for ternary oxides.** Differences between corrected and experimental room temperature formation enthalpies of 71 ternary oxides for SCAN. In addition to the CCE results, a comparison to an implementation of the FERE method [25] for our dataset (quasi-FERE) [32] is also included. The red lines at ± 50 meV/atom indicate the typical MAE of previous correction schemes [26, 27]. Adapted from Ref. 32.

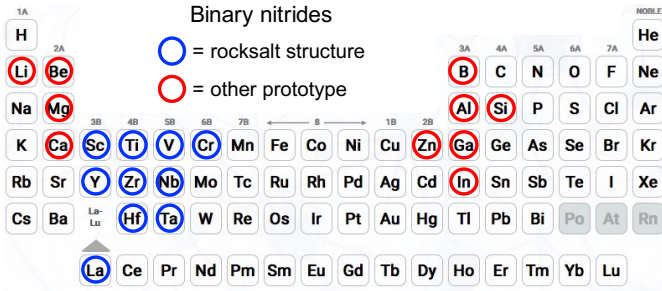


FIG. 4. **Phase space of binary nitrides.** Periodic table with elements forming binary nitrides for which validated thermochemical data are available in standard collections [33–36] highlighted by circles. Blue indicates the formation of rock salt structures and red stands for other structural prototypes.

tional efforts have therefore also been devoted to predict metastable nitrides from suitable reactive nitrogen precursors [67] and to build large stability maps of the uncharted nitrides materials space [68]. We note that in the set of known binaries in Fig. 4 there is a predominance of rock salt structures indicated in blue as all *d*-element nitrides except Zn_3N_2 crystallize in this prototype. These are expected to be very suitable precursors for high-entropy systems since many high-entropy carbides and oxides have this structure [17, 69].

Figure 5 shows the difference between calculated DFT+AGL and experimental room temperature formation enthalpies, as well as the vibrational contribution in the lower panel. The MAEs for the nitrides are generally

larger as for the oxides with PBE again mostly underestimating the enthalpies with respect to experiment while LDA and SCAN typically lead to an overestimation. Although there has been some debate about whether the tabulated experimental $\Delta_f H$ for GaN [33] should be updated with a more negative value [25, 70], we stick to the old result since only in this case it fits to the overall behavior that LDA and SCAN overestimate the formation enthalpy whereas PBE does the opposite as observed for BN, AlN, and InN. With the small vibrational contribution being at max of the order of 10-20 meV/atom with no significant differences between the approximations, the main error arises once more from the internal (DFT) energy contribution. Over the whole set, the three functionals exhibit significant MAEs of 161, 229, and 155 meV/atom for PBE, LDA, and SCAN, respectively outlining again the meta-GGA as most accurate. There is nevertheless a strong dependence on the *l*-character of the cation species. While for the *s*-element nitrides, SCAN exhibits the by far smallest MAE of 69 meV/atom, PBE performs best for the *p*-compounds and yields about the same average error as SCAN for the *d*-systems. LDA shows the largest errors for all three groups in strict contrast to the oxides where it is significantly better than PBE and, for the ternaries, even close to SCAN. Thus, this success of LDA is not systematic for all materials classes. It should be noted that, compared to the oxides, where the experimental errorbar is likely on the order of 10-20 meV/atom [32], the average error of the Kubaschewski values [33] given for all binaries except TiN is ~ 33 meV/atom.

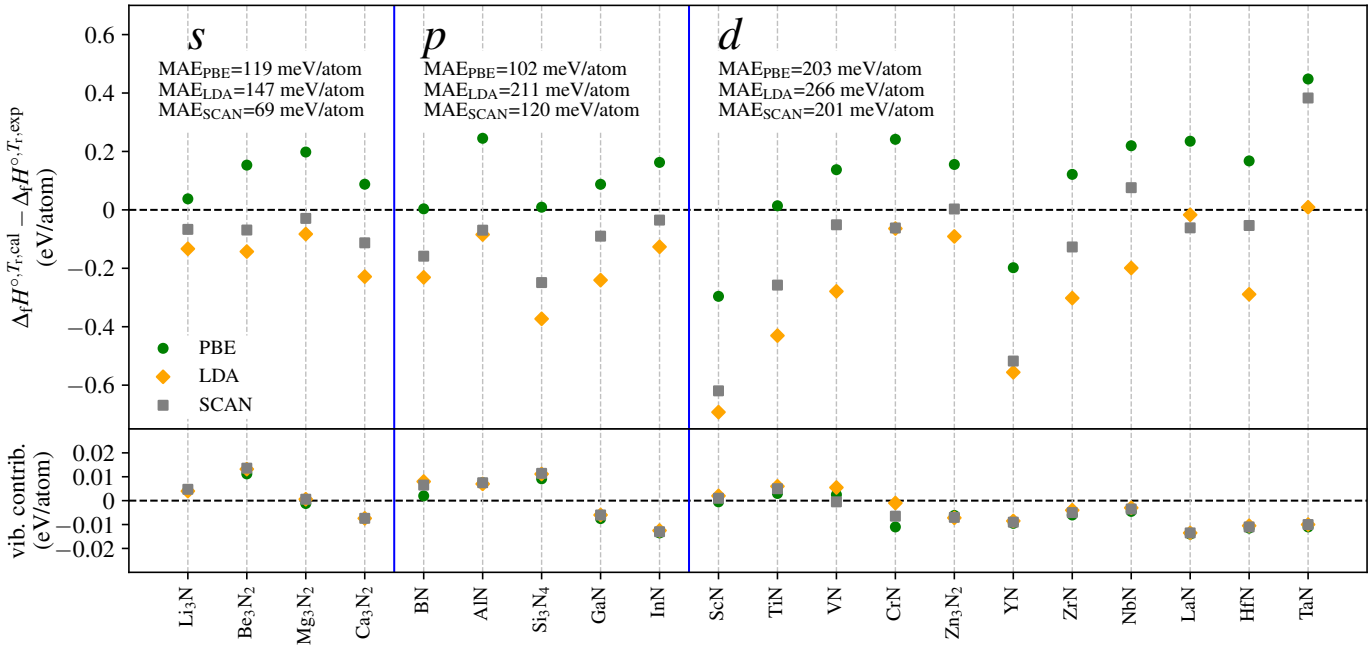


FIG. 5. **Formation enthalpies and vibrational contribution for binary nitrides.** Differences between calculated and experimental room temperature formation enthalpies of 20 binary nitrides (upper panel) and vibrational (zero-point + thermal) contribution to the calculated formation enthalpy (lower panel) for three standard DFT functionals. Vertical blue lines separate blocks with different l -character of the cations.

TABLE I: **CCE corrections for 298.15 and 0 K for nitrides.** Corrections per bond $\delta H_{A-Y}^{T,A+\alpha}$ of the CCE method for each cation species A in oxidation states $+\alpha$ for 298.15 and 0 K obtained from binary nitrides for the different functionals. The experimental formation enthalpies per bond that can be used to obtain a rough estimate of the $\Delta_f H$ value of a material without DFT calculations according to Ref. 32 and 49, are given in the last column. All corrections are in eV/bond.

cation species A	$+\alpha$	PBE		LDA		SCAN		CCE@exp
		298.15 K	0 K	298.15 K	0 K	298.15 K	0 K	298.15 K
Li	+1	0.01663	0.00912	-0.06850	-0.07562	-0.03588	-0.04338	-0.21350
Be	+2	0.05908	0.05292	-0.06500	-0.07133	-0.03433	-0.04075	-0.50917
B	+3	0.00100	-0.00867	-0.15933	-0.17000	-0.11000	-0.12067	-0.86700
Mg	+2	0.08300	0.07642	-0.03475	-0.04167	-0.01242	-0.01950	-0.39858
Al	+3	0.11875	0.10850	-0.04575	-0.05575	-0.03850	-0.04875	-0.82500
Si	+4	0.00000	-0.01300	-0.22408	-0.23733	-0.15183	-0.16508	-0.64325
Ca	+2	0.03967	0.03400	-0.09225	-0.09792	-0.04392	-0.04942	-0.37225
Sc	+3	-0.09850	-0.10500	-0.23150	-0.23833	-0.20667	-0.21350	-0.54200
Ti	+3	0.00367	-0.00283	-0.14550	-0.15233	-0.08733	-0.09400	-0.58400
V	+3	0.04500	0.03917	-0.09483	-0.10100	-0.01683	-0.02250	-0.37650
Cr	+3	0.08417	0.08167	-0.02100	-0.02583	-0.01867	-0.02233	-0.20250
Zn	+2	0.06733	0.06225	-0.03492	-0.03908	0.00417	-0.00025	-0.01950
Ga	+3	0.04725	0.03950	-0.11725	-0.12550	-0.04200	-0.05075	-0.28400
Y	+3	-0.06283	-0.06750	-0.18267	-0.18783	-0.16950	-0.17450	-0.51683
Zr	+3	0.04250	0.03733	-0.09933	-0.10500	-0.04067	-0.04617	-0.63100
Nb	+3	0.07467	0.06967	-0.06550	-0.07083	0.02667	0.02150	-0.40833
In	+3	0.08825	0.08350	-0.05700	-0.06225	-0.01125	-0.01650	-0.04450
La	+3	0.08300	0.07983	-0.00100	-0.00433	-0.01600	-0.01950	-0.52400
Hf	+3	0.05983	0.05633	-0.09283	-0.09683	-0.01433	-0.01817	-0.64533
Ta	+3	0.15283	0.14933	0.00617	0.00233	0.13100	0.12733	-0.43583

The results from the binaries are then used to obtain the CCE corrections for nitrides which are listed in Table I including also the experimental formation enthalpies per bond CCE@exp [32, 49]. As shown by us previously in Refs. 32 and 49, the vibrational contribution does not need to be taken into account explicitly and the correc-

tions can be directly fitted to the plain DFT formation enthalpies. This gives two types of corrections: (i) for room temperature (298.15 K) and (ii) for 0 K, meaning that when they are applied to the plain DFT enthalpies of target compounds, they yield corrected estimates for the respective temperature.

The amount of ternary nitrides in particular with validated thermochemical and structural data which are also available in the AFLOW-ICSD database is, however, very scarce, with no entries in the standard collections that were used for the oxides. In Fig. 6 we present both the uncorrected and corrected results for three compounds with measured formation enthalpies reported in Refs. [71, 72]. As expected, the plain DFT results show large errors for all three functionals (MAEs of 85, 162, and 88 meV/atom for PBE, LDA, and SCAN). When CCE is applied, the MAEs reduce to 16, 18, and 21 meV/atom again confirming the high accuracy of CCE enthalpies although of course average values for a set of only three entries must be taken with some care.

The oxide and nitride corrections are available from the AFLOW-CCE module which automatically determines the oxidation numbers of all ions and only needs a structure as input [49]. It has been integrated into the AFLOW software [4] of version 3.2.7 or later for which the source code is available at <http://aflow.org/install-aflow/> and <http://materials.duke.edu/AFLOW/>. The implementation also includes a Python environment that is distributed with the AFLOW source and can be generated with the command `aflow --cce --print=python`. The CCE web tool [5] can be accessed via: <http://aflow.org/aflow-online/>. The main commands for the AFLOW-CCE command line tool are summarized in Table II. Instructions are available through the AFLOW-School: <http://aflow.org/aflow-school/>. All options and further details are described in Ref. [49].

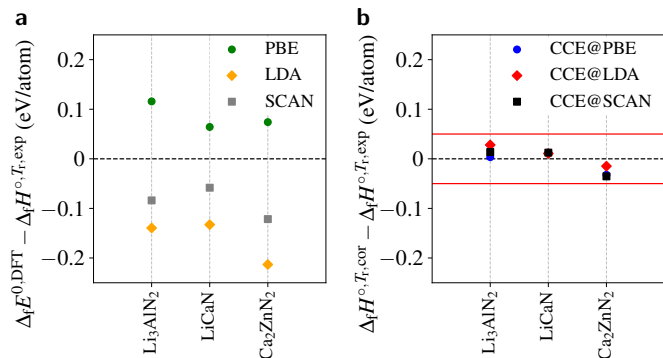


FIG. 6. **Uncorrected and corrected enthalpies for ternary nitrides.** Differences between calculated (a) as well as corrected (b) and experimental room temperature formation enthalpies for seven ternary nitrides. The red lines at ± 50 meV/atom indicate the typical MAE of previous correction schemes [26, 27].

Future implementations. The CCE parameterization will be extended to all other relevant anion classes. These include: (i) all halides, *i.e.* fluorides, chlorides, bromides, and iodides; (ii) all additional chalcogenides, *i.e.* sulfides, selenides, and tellurides; (iii) additional pnictides, *i.e.* phosphides, arsenides, and potentially antimonides; and (iv) possibly hydrides. The method will also be lever-

aged for the challenging design of disordered high-entropy ceramics by providing an ensemble of corrections for the partial occupation (AFLOW-POCC) [64] algorithm used to model these materials. It is also expected to become very useful for energetic corrections of nanostructures and in surface science based on the bonding topology, where for instance, the relative stability of different quasi 2D systems and with respect to bulk materials [19–23] must be estimated accurately. The temperature dependence can be implemented in a dynamic fashion allowing for enthalpy estimates at any given temperature on the fly.

CONCLUSIONS

We have presented the computational capabilities of the AFLOW-CCE software for thermodynamic stability predictions utilizing our previous oxide data and new results for nitrides. When calculating the formation enthalpies from plain DFT for several standard functionals such as LDA, PBE, and SCAN, average errors compared to high-quality experimental data of the order of several hundred meV/atom are found. For oxides, SCAN shows the best performance achieving ~ 100 meV/atom closely followed by LDA. Also for nitrides, SCAN depicts the smallest mean errors slightly above 150 meV/atom almost matched by PBE with LDA revealing larger deviations.

Since the accuracy of these approximations is too low for materials design at room temperature (~ 25 meV), we employ the AFLOW-CCE implementation of our previously developed coordination corrected enthalpies method for the accurate evaluation of the thermodynamic stability of ionic materials. CCE is based on an intuitive parametrization of DFT errors with respect to coordination numbers and cation oxidation states. The method has been benchmarked for the formation enthalpies of oxides and nitrides revealing mean errors on the order of ~ 25 meV/atom. In addition, it can rectify errors in relative stability predictions of polymorphs from plain DFT. The corrections are freely available in the AFLOW-CCE module for the automatic correction of enthalpies based on only structural inputs. The method and its implementation can be valuable for correcting the results in large materials databases to enable advanced materials predictions.

ACKNOWLEDGMENTS

The authors thank David Hicks, Cormac Toher, Ohad Levy, Simon Divilov, Hagen Eckert, Michael Mehl, Adam Zettel, Corey Oses, Arrigo Calzolari, Arkady V. Krashennnikov, Thomas Heine, and Xiomara Campilongo for fruitful discussions. S.C. acknowledges the DoD SPICES MURI sponsored by the Office of Naval Research (Naval Research contract N00014-21-1-2515) for financial

TABLE II. Main commands for the AFLOW-CCE command line tool.

Command	Description
<code>aflow --cce</code>	Prints user instructions.
<code>aflow --cce=STRUCTURE_FILE_PATH</code>	Provides the output of the full CCE analysis, <i>i.e.</i> cation coordination numbers, oxidation numbers, and CCE corrections and formation enthalpies, for the structure in STRUCTURE_FILE_PATH.
<code>aflow --get_cce_corrections < STRUCTURE_FILE_PATH</code>	Returns the CCE corrections and formation enthalpies for the structure in STRUCTURE_FILE_PATH.
<code>aflow --get_oxidation_number < STRUCTURE_FILE_PATH</code>	Gives the oxidation numbers for the structure in STRUCTURE_FILE_PATH.
<code>aflow --get_cation_coord_num < STRUCTURE_FILE_PATH</code>	Determines the cation coordination numbers for the structure in STRUCTURE_FILE_PATH.

support. R.F. acknowledges funding for the ‘‘Autonomous Materials Thermodynamics’’ (AutoMaT) project by Technische Universitat Dresden and Helmholtz-Zentrum Dresden-Rossendorf within the DRESDEN-concept alliance. R.F. acknowledges support from the Alexander

von Humboldt foundation under the Feodor Lynen research fellowship. The authors thank the HZDR Computing Center, HLRS Stuttgart (HAWK cluster), the Paderborn Center for Parallel Computing (PC2, Noctua 2 cluster), and the DoD High Performance Computing Modernization Program for computational support.

Appendix A: Tables with numerical data

TABLE III: **Structural data for binary and ternary nitrides.** ICSD numbers, space group numbers, Pearson symbols, and AFLOW prototype labels [73–75] for the 20 binary and three ternary nitrides. Space-groups and Pearson symbols are calculated with AFLOW-SYM [76]. Note: the order of the Wyckoff position letters in the prototype column follows the alphabetic syntax to generate the prototype, while the associated web-link points to the standardized description in the AFLOW Encyclopedia of Crystallographic Prototypes [73–75].

formula	ICSD #	space group #	Pearson symbol	AFLOW prototype
Li ₃ N	76944	191	hP4	A3B_hP4_191_bc_a
Be ₃ N ₂	616348	206	cI80	A3B2_cI80_206_e_bd
Mg ₃ N ₂	411210	206	cI80	A3B2_cI80_206_e_bd
Ca ₃ N ₂	50991	206	cI80	A3B2_cI80_206_e_bd
BN	186246	194	hP4	AB_hP4_194_d_c
AlN	602459	186	hP4	AB_hP4_186_b_b
Si ₃ N ₄	74744	176	hP14	A4B3_hP14_176_ch_h
GaN	156259	186	hP4	AB_hP4_186_b_b
InN	157515	186	hP4	AB_hP4_186_b_b
ScN	26948	225	cF8	AB_cF8_225_b_a
TiN	64907	225	cF8	AB_cF8_225_b_a
VN	76526	225	cF8	AB_cF8_225_b_a
CrN	41827	225	cF8	AB_cF8_225_a_b
Zn ₃ N ₂	84918	206	cI80	A2B3_cI80_206_ad_e
YN	76528	225	cF8	AB_cF8_225_b_a
ZrN	167851	225	cF8	AB_cF8_225_a_b
NbN	183423	225	cF8	AB_cF8_225_b_a
LaN	641462	225	cF8	AB_cF8_225_a_b
HfN	53025	225	cF8	AB_cF8_225_a_b
TaN	644727	225	cF8	AB_cF8_225_b_a
Li ₃ AlN ₂	25565	206	cI96	AB3C2_cI96_206_c_e_bd
LiCaN	107304	62	oP12	ABC_oP12_62_c_c_c
Ca ₂ ZnN ₂	69049	139	tI10	A2B2C_tI10_139_e_e_a

TABLE IV: **Formation enthalpies for binary and ternary nitrides.** Calculated DFT+AGL, plain DFT and experimental room temperature formation enthalpies, number of cation-anion bonds N_{A-Y} per formula unit and oxidation states $+α$ of the cation(s) for binary and ternary nitrides. In case of ternaries, for the cation-nitrogen bonds- and oxidation numbers, the first (second) number in the column refers to the first (second) element in the formula. Experimental values are from Kubaschewski *et al.* [33], NIST-JANAF [34], Barin [35], and McHale *et al.* [71, 72]. Enthalpies are in eV/atom; corrections are in eV/bond.

formula	PBE+AGL	PBE	LDA+AGL	LDA	SCAN+AGL	SCAN	Exp.	N_{A-Y}	$+α$
Li ₃ N	-0.389	-0.394	-0.560	-0.564	-0.494	-0.499	-0.427 [33]	8	+1
Be ₃ N ₂	-1.069	-1.080	-1.365	-1.378	-1.291	-1.304	-1.222 [33]	12	+2
Mg ₃ N ₂	-0.759	-0.757	-1.039	-1.040	-0.986	-0.986	-0.957 [33]	12	+2
Ca ₃ N ₂	-0.806	-0.798	-1.122	-1.115	-1.006	-0.999	-0.893 [35]	12	+2
BN	-1.297	-1.299	-1.532	-1.539	-1.459	-1.466	-1.300 [34]	3	+3
AlN	-1.405	-1.413	-1.735	-1.742	-1.719	-1.727	-1.650 [33]	4	+3
Si ₃ N ₄	-1.094	-1.103	-1.476	-1.487	-1.352	-1.363	-1.103 [33]	12	+4
GaN	-0.481	-0.473	-0.808	-0.802	-0.658	-0.652	-0.568 [33]	4	+3
InN	0.074	0.087	-0.215	-0.203	-0.124	-0.111	-0.089 [35]	4	+3
ScN	-1.922	-1.922	-2.318	-2.320	-2.245	-2.246	-1.626 [33]	6	+3
TiN	-1.738	-1.741	-2.182	-2.188	-2.009	-2.014	-1.752 [33]	6	+3
VN	-0.992	-0.994	-1.408	-1.414	-1.180	-1.180	-1.129 [33]	6	+3
CrN	-0.366	-0.355	-0.672	-0.670	-0.670	-0.663	-0.608 [33]	6	+3
Zn ₃ N ₂	0.109	0.115	-0.138	-0.131	-0.044	-0.037	-0.047 [33]	12	+2
YN	-1.749	-1.739	-2.107	-2.098	-2.068	-2.059	-1.550 [33]	6	+3
ZrN	-1.771	-1.765	-2.195	-2.191	-2.020	-2.015	-1.893 [34]	6	+3
NbN	-1.006	-1.001	-1.424	-1.421	-1.149	-1.145	-1.225 [33]	6	+3
LaN	-1.337	-1.323	-1.589	-1.575	-1.634	-1.620	-1.572 [35]	6	+3
HfN	-1.768	-1.757	-2.225	-2.215	-1.990	-1.979	-1.936 [33]	6	+3
TaN	-0.860	-0.849	-1.299	-1.289	-0.924	-0.914	-1.308 [33]	6	+3
Li ₃ AlN ₂	-0.853	-0.865	-1.109	-1.120	-1.053	-1.065	-0.981 [72]	12, 4	+1, +3
LiCaN	-0.667	-0.663	-0.929	-0.926	-0.830	-0.827	-0.562 [71]	3, 4	+1, +2
Ca ₂ ZnN ₂	-0.718	-0.711	-1.006	-0.999	-0.914	-0.907	-0.785 [71]	10, 2	+2, +2

TABLE V: **AGL contributions to the formation enthalpies for binary and ternary nitrides.** Total vibrational (TVC), zero-point (ZPC) and thermal (TC) contributions to the calculated formation enthalpies obtained from AGL [50–54] for each functional for binary and ternary nitrides. The sum of ZPC and TC might not match exactly the total AGL contribution listed due to rounding. All values are in eV/atom.

formula	PBE			LDA			SCAN		
	AGL-TVC	AGL-ZPC	AGL-TC	AGL-TVC	AGL-ZPC	AGL-TC	AGL-TVC	AGL-ZPC	AGL-TC
Li ₃ N	0.004	0.019	-0.015	0.004	0.018	-0.014	0.005	0.020	-0.015
Be ₃ N ₂	0.011	0.026	-0.015	0.013	0.028	-0.015	0.014	0.029	-0.015
Mg ₃ N ₂	-0.001	0.015	-0.016	0.001	0.017	-0.017	0.001	0.017	-0.017
Ca ₃ N ₂	-0.007	0.006	-0.014	-0.007	0.006	-0.014	-0.007	0.006	-0.013
BN	0.002	0.017	-0.015	0.008	0.024	-0.016	0.007	0.022	-0.016
AlN	0.007	0.028	-0.021	0.007	0.027	-0.020	0.007	0.028	-0.021
Si ₃ N ₄	0.009	0.031	-0.022	0.011	0.034	-0.023	0.011	0.034	-0.023
GaN	-0.007	0.008	-0.016	-0.006	0.010	-0.016	-0.006	0.012	-0.018
InN	-0.014	-0.004	-0.009	-0.013	-0.002	-0.010	-0.013	-0.002	-0.011
ScN	0.000	0.019	-0.020	0.002	0.023	-0.021	0.001	0.021	-0.020
TiN	0.003	0.022	-0.019	0.006	0.026	-0.020	0.005	0.025	-0.020
VN	0.002	0.020	-0.018	0.006	0.024	-0.019	0.000	0.017	-0.017
CrN	-0.011	-0.004	-0.008	-0.001	0.014	-0.015	-0.006	0.005	-0.011
Zn ₃ N ₂	-0.006	0.006	-0.012	-0.007	0.003	-0.010	-0.007	0.004	-0.011
YN	-0.010	0.004	-0.014	-0.008	0.007	-0.015	-0.009	0.006	-0.015
ZrN	-0.006	0.010	-0.016	-0.004	0.013	-0.017	-0.005	0.011	-0.016
NbN	-0.005	0.010	-0.015	-0.003	0.013	-0.016	-0.004	0.012	-0.016
LaN	-0.014	-0.005	-0.009	-0.014	-0.003	-0.010	-0.014	-0.003	-0.011
HfN	-0.012	-0.001	-0.011	-0.011	0.001	-0.012	-0.011	0.001	-0.012
TaN	-0.011	-0.001	-0.010	-0.010	0.002	-0.011	-0.010	0.001	-0.011
Li ₃ AlN ₂	0.012	0.032	-0.021	0.011	0.031	-0.020	0.012	0.033	-0.021
LiCaN	-0.003	0.010	-0.013	-0.003	0.010	-0.013	-0.003	0.010	-0.013
Ca ₂ ZnN ₂	-0.007	0.006	-0.013	-0.007	0.005	-0.012	-0.007	0.005	-0.012

TABLE VI: **CCE formation enthalpies for ternary nitrides.** CCE formation enthalpies (using the corrections from Table I) and experimental room temperature values for ternary nitrides. Experimental data are from McHale *et al.* [71, 72]. All enthalpies are in eV/atom.

formula	CCE@ PBE	CCE@ LDA	CCE@ SCAN	Exp.
Li ₃ AlN ₂	-0.978	-0.953	-0.967	-0.981 [72]
LiCaN	-0.550	-0.551	-0.549	-0.562 [71]
Ca ₂ ZnN ₂	-0.818	-0.800	-0.821	-0.785 [71]

- [1] J. P. Perdew and A. Zunger, *Self-interaction correction to density-functional approximations for many-electron systems*, Phys. Rev. B **23**, 5048–5079 (1981), doi:10.1103/PhysRevB.23.5048.
- [2] J. P. Perdew, K. Burke, and M. Ernzerhof, *Generalized Gradient Approximation Made Simple*, Phys. Rev. Lett. **77**, 3865–3868 (1996), doi:10.1103/PhysRevLett.77.3865.
- [3] J. Sun, A. Ruzsinszky, and J. P. Perdew, *Strongly Constrained and Appropriately Normed Semilocal Density Functional*, Phys. Rev. Lett. **115**, 036402 (2015), doi:10.1103/PhysRevLett.115.036402.
- [4] C. Oses, M. Esters, D. Hicks, S. Divilov, H. Eckert, R. Friedrich, M. J. Mehl, A. Smolyanyuk, X. Campilongo, A. van de Walle, J. Schroers, A. G. Kusne, I. Takeuchi, E. Zurek, M. Buongiorno Nardelli, M. Fornari, Y. Lederer, O. Levy, C. Toher, and S. Curtarolo, *afLOW++: A C++ framework for autonomous materials design*, Comput. Mater. Sci. **217**, 111889 (2023), doi:10.1016/j.commatsci.2022.111889.
- [5] M. Esters, C. Oses, S. Divilov, H. Eckert, R. Friedrich, D. Hicks, M. J. Mehl, F. Rose, A. Smolyanyuk, A. Calzolari, X. Campilongo, C. Toher, and S. Curtarolo, *afLOW.org: A web ecosystem of databases, software and tools*, Comput. Mater. Sci. **216**, 111808 (2023), doi:10.1016/j.commatsci.2022.111808.
- [6] S. Curtarolo, W. Setyawan, S. Wang, J. Xue, K. Yang, R. H. Taylor, L. J. Nelson, G. L. W. Hart, S. Sanvito, M. Buongiorno Nardelli, N. Mingo, and O. Levy, *AFLOWLIB.ORG: A distributed materials properties repository from high-throughput ab initio calculations*, Comput. Mater. Sci. **58**, 227–235 (2012), doi:10.1016/j.commatsci.2012.02.002.
- [7] A. Jain, G. Hautier, C. J. Moore, S. P. Ong, C. C. Fischer, T. Mueller, K. A. Persson, and G. Ceder, *A high-throughput infrastructure for density functional theory calculations*, Comput. Mater. Sci. **50**, 2295–2310 (2011), doi:10.1016/j.commatsci.2011.02.023.
- [8] J. E. Saal, S. Kirklin, M. Aykol, B. Meredig, and C. Wolverton, *Materials Design and Discovery with High-Throughput Density Functional Theory: The Open Quantum Materials Database (OQMD)*, JOM **65**, 1501–1509 (2013), doi:10.1007/s11837-013-0755-4.
- [9] S. Kirklin, J. E. Saal, B. Meredig, A. Thompson, J. W. Doak, M. Aykol, S. Rühl, and C. Wolverton, *The Open Quantum Materials Database (OQMD): assessing the accuracy of DFT formation energies*, npj Comput. Mater. **1**, 15010 (2015), doi:10.1038/npjcompumats.2015.10.
- [10] C. Draxl and M. Scheffler, *NOMAD: The FAIR concept for big data-driven materials science*, MRS Bull. **43**, 676–682 (2018), doi:10.1557/mrs.2018.208.
- [11] S. R. Bahn and K. W. Jacobsen, *An object-oriented scripting interface to a legacy electronic structure code*, Comput. Sci. Eng. **4**, 56–66 (2002), doi:10.1109/5992.998641.
- [12] D. D. Landis, J. S. Hummelshøj, S. Nestorov, J. Greeley, M. Dulak, T. Bligaard, J. K. Nørskov, and K. W. Jacobsen, *The Computational Materials Repository*, Comput. Sci. Eng. **14**, 51–57 (2012), doi:10.1109/MCSE.2012.16.
- [13] G. Pizzi, A. Cepellotti, R. Sabatini, N. Marzari, and B. Kozinsky, *AiiDA: automated interactive infrastructure and database for computational science*, Comput. Mater. Sci. **111**, 218–230 (2016).
- [14] P. A. M. Dirac, *Quantum Mechanics of Many-Electron Systems*, Proc. R. Soc. A Math. Phys. Eng. Sci. **123**, 714–733 (1929), doi:10.1098/rspa.1929.0094.
- [15] M. J. Mehl, M. Ronquillo, D. Hicks, M. Esters, C. Oses, R. Friedrich, A. Smolyanyuk, E. Gossett, D. Finkenshtadt, and S. Curtarolo, *The Tin Pest Problem as a Test of Density Functionals Using High-Throughput Calculations*, Phys. Rev. Materials **5**, 083608 (2021), doi:10.1103/PhysRevMaterials.5.083608.
- [16] P. Sarker, T. Harrington, et al., *High-entropy high-hardness metal carbides discovered by entropy descriptors*, Nat. Commun. **9**, 4980 (2018), doi:10.1038/s41467-018-07160-7.
- [17] C. Oses, C. Toher, and S. Curtarolo, *High-entropy ceramics*, Nat. Rev. Mater. **5**, 295–309 (2020), doi:10.1038/s41578-019-0170-8.
- [18] J. Gil and T. Oda, *Correction methods for first-principles calculations of the solution enthalpy of gases and compounds in liquid metals*, Phys. Chem. Chem. Phys. **24**, 757–770 (2022), doi:10.1039/D1CP02450G.
- [19] A. Puthirath Balan, S. Radhakrishnan, C. F. Woellner, S. K. Sinha, L. Deng, C. d. l. Reyes, B. M. Rao, M. Paulose, R. Neupane, A. Apte, V. Kochat, R. Vajtai, A. R. Harutyunyan, C.-W. Chu, G. Costin, D. S. Galvao, A. A. Martí, P. A. van Aken, O. K. Varghese, C. S. Tiwary, A. Malie Madom Ramaswamy Iyer, and P. M. Ajayan, *Exfoliation of a non-van der Waals material from iron ore hematite*, Nat. Nanotechnol. **13**, 602–609 (2018), doi:10.1038/s41565-018-0134-y.
- [20] R. Friedrich, M. Ghorbani-Asl, S. Curtarolo, and A. V. Krasheninnikov, *Data-Driven Quest for Two-Dimensional Non-van der Waals Materials*, Nano Lett. **22**, 989–997 (2022), doi:10.1021/acs.nanolett.1c03841.
- [21] T. Barnowsky, A. V. Krasheninnikov, and R. Friedrich, *A New Group of 2D Non-van der Waals Materials with Ultra Low Exfoliation Energies*, Adv. Electron. Mater. **9**, 2201112 (2023), doi:10.1002/aelm.202201112.
- [22] A. P. Balan, A. B. Puthirath, S. Roy, G. Costin, E. F. Oliveira, M. A. S. R. Saadi, V. Sreepal, R. Friedrich,

- P. Serles, A. Biswas, S. A. Iyengar, N. Chakingal, S. Bhat-tacharyya, S. K. Saju, S. C. Pardo, L. M. Sassi, T. Fil-leter, A. Krasheninikov, D. S. Galvao, R. Vajtai, R. R. Nair, and P. M. Ajayan, *Non-van der Waals quasi-2D materials; recent advances in synthesis, emergent prop-erties and applications*, Mater. Today **58**, 164 (2022), doi: 10.1016/j.mattod.2022.07.007.
- [23] H. Kaur and J. N. Coleman, *Liquid-Phase Exfolia-tion of Nonlayered Non-Van-Der-Waals Crystals into Nanoplatelets*, Adv. Mater. **34**, 2202164 (2022), doi: 10.1002/adma.202202164.
- [24] L. Wang, T. Maxisch, and G. Ceder, *Oxidation en-ergies of transition metal oxides within the GGA+U framework*, Phys. Rev. B **73**, 195107 (2006), doi: 10.1103/PhysRevB.73.195107.
- [25] S. Lany, *Semiconductor thermochemistry in density func-tional calculations*, Phys. Rev. B **78**, 245207 (2008), doi: 10.1103/PhysRevB.78.245207.
- [26] A. Jain, G. Hautier, S. P. Ong, C. J. Moore, C. C. Fischer, K. A. Persson, and G. Ceder, *Formation enthalpies by mixing GGA and GGA+U calculations*, Phys. Rev. B **84**, 045115 (2011), doi:10.1103/PhysRevB.84.045115.
- [27] V. Stevanović, S. Lany, X. Zhang, and A. Zunger, *Cor-recting density functional theory for accurate predictions of compound enthalpies of formation: Fitted elemental-phase reference energies*, Phys. Rev. B **85**, 115104 (2012), doi:10.1103/PhysRevB.85.115104.
- [28] J. Yan, J. S. Hummelshøj, and J. K. Nørskov, *Forma-tion energies of group I and II metal oxides using random phase approximation*, Phys. Rev. B **87**, 075207 (2013), doi:10.1103/PhysRevB.87.075207.
- [29] T. S. Jauho, T. Olsen, T. Bligaard, and K. S. Thyge-sen, *Improved description of metal oxide stability: Be-yond the random phase approximation with renormal-ized kernels*, Phys. Rev. B **92**, 115140 (2015), doi: 10.1103/PhysRevB.92.115140.
- [30] Y. Zhang, D. A. Kitchaev, J. Yang, T. Chen, S. T. Dacek, R. A. Sarmiento-Pérez, M. A. L. Marques, H. Peng, G. Ceder, J. P. Perdew, and J. Sun, *Efficient first-principles prediction of solid stability: Towards chem-ical accuracy*, npj Comput. Mater. **4**, 9 (2018), doi: 10.1038/s41524-018-0065-z.
- [31] E. B. Isaacs and C. Wolverton, *Performance of the strongly constrained and appropriately normed density functional for solid-state mate-rials*, Phys. Rev. Materials **2**, 063801 (2018), doi: 10.1103/PhysRevMaterials.2.063801.
- [32] R. Friedrich, D. Usanmaz, C. Oses, A. Supka, M. Fornari, M. Buongiorno Nardelli, C. Toher, and S. Curtarolo, *Co-ordination corrected ab initio formation enthalpies*, npj Comput. Mater. **5**, 59 (2019), doi:10.1038/s41524-019-0192-1.
- [33] O. Kubaschewski, C. B. Alcock, and P. J. Spencer, *Ma-terials Thermochemistry* (Pergamon Press, Oxford, UK, 1993), 6th edn.
- [34] M. W. Chase, Jr., *NIST-JANAF Thermochemical Tables* (American Chemical Society and American Institute of Physics for the National Institute of Standards and Tech-nology, Woodbury, NY, 1998), 4th edn.
- [35] I. Barin, *Thermochemical Data of Pure Substances* (VCH, Weinheim, 1995), 3rd edn.
- [36] D. D. Wagman, W. H. Evans, V. B. Parker, R. H. Schumm, I. Halow, S. M. Bailey, K. L. Churney, and R. L. Nuttall, *The NBS tables of chemical thermodynamic prop-erties*, J. Phys. Chem. Ref. Data **11**, Supplement No. 2 (1982).
- [37] M. R. Pederson, A. Ruzsinszky, and J. P. Perdew, *Com-munication: Self-interaction correction with unitary in-variance in density functional theory*, J. Chem. Phys. **140**, 121103 (2014), doi:10.1063/1.4869581.
- [38] Z.-h. Yang, M. R. Pederson, and J. P. Perdew, *Full self-consistency in the Fermi-orbital self-interaction correction*, Phys. Rev. A **95**, 052505 (2017), doi: 10.1103/PhysRevA.95.052505.
- [39] D.-y. Kao, K. Withanage, T. Hahn, J. Batool, J. Kor-tus, and K. Jackson, *Self-consistent self-interaction cor-rected density functional theory calculations for atoms us-ing Fermi-Löwdin orbitals: Optimized Fermi-orbital de-scriptors for Li-Kr*, J. Chem. Phys. **147**, 164107 (2017), doi:10.1063/1.4996498.
- [40] S. Schwalbe, T. Hahn, S. Liebing, K. Treppe, and J. Kor-tus, *Fermi-Löwdin Orbital Self-interaction Corrected Den-sity Functional Theory: Ionization Potentials and En-thalpies of Formation*, J. Comput. Chem. **39**, 2463–2471 (2018), doi:10.1002/jcc.25586.
- [41] M. Pozzo and D. Alfé, *Structural properties and enthalpy of formation of magnesium hydride from quantum Monte Carlo calculations*, Phys. Rev. B **77**, 104103 (2008), doi: 10.1103/PhysRevB.77.104103.
- [42] G. Mao, X. Hu, X. Wu, Y. Dai, S. Chu, and J. Deng, *Benchmark Quantum Monte Carlo calcu-lation of the enthalpy of formation of MgH₂*, Int. J. of Hydrogen Energy **36**, 8388–8391 (2011), doi: 10.1016/j.ijhydene.2011.04.093.
- [43] E. B. Isaacs, H. Shin, A. Annaberdiyev, C. Wolverton, L. Mitas, A. Benali, and O. Heinonen, *Assessing the accuracy of compound formation energies with quantum Monte Carlo*, Phys. Rev. B **105**, 224110 (2022), doi: 10.1103/PhysRevB.105.224110.
- [44] A. Wang, R. Kingsbury, M. McDermott, M. Horton, A. Jain, S. P. Ong, S. Dwaraknath, and K. A. Persson, *A framework for quantifying uncertainty in DFT energy cor-rections*, Sci. Rep. **11**, 15496 (2021), doi:10.1038/s41598-021-94550-5.
- [45] M. Aykol and C. Wolverton, *Local environment dependent GGA+U method for accurate thermochemistry of transi-tion metal compounds*, Phys. Rev. B **90**, 115105 (2014), doi:10.1103/PhysRevB.90.115105.
- [46] N. Artrith, J. A. Garrido Torres, A. Urban, and M. S. Hy-bertsen, *Data-driven approach to parameterize SCAN+U for an accurate description of 3d transition metal oxide thermochemistry*, Phys. Rev. Materials **6**, 035003 (2022), doi:10.1103/PhysRevMaterials.6.035003.
- [47] R. S. Kingsbury, A. S. Rosen, A. S. Gupta, J. M. Munro, S. P. Ong, A. Jain, S. Dwaraknath, M. K. Horton, and K. A. Persson, *A flexible and scalable scheme for mixing computed formation energies from different lev-els of theory*, npj Comput. Mater. **8**, 195 (2022), doi: 10.1038/s41524-022-00881-w.
- [48] S. Gong, S. Wang, T. Xie, W. H. Chae, R. Liu, Y. Shao-Horn, and J. C. Grossman, *Calibrating DFT Formation Enthalpy Calculations by Multifidelity Ma-chine Learning*, JACS Au **2**, 1964–1977 (2022), doi: 10.1021/jacsau.2c00235.
- [49] R. Friedrich, M. Esters, C. Oses, S. Ki, M. J. Bren-ner, D. Hicks, M. J. Mehl, C. Toher, and S. Cur-tarolo, *Automated coordination corrected enthalpies with AFLOW-CCE*, Phys. Rev. Materials **5**, 043803 (2021),

- doi:10.1103/PhysRevMaterials.5.043803.
- [50] M. A. Blanco, A. M. Pendás, E. Francisco, J. M. Recio, and R. Franco, *Thermodynamical properties of solids from microscopic theory: Applications to MgF₂ and Al₂O₃*, J. Mol. Struct.: Theochem **368**, 245–255 (1996), doi:10.1016/S0166-1280(96)90571-0.
- [51] M. A. Blanco, E. Francisco, and V. Luaña, *GIBBS: isothermal-isobaric thermodynamics of solids from energy curves using a quasi-harmonic Debye model*, Comput. Phys. Commun. **158**, 57–72 (2004), doi:10.1016/j.comphy.2003.12.001.
- [52] C. Toher, J. J. Plata, O. Levy, M. de Jong, M. Asta, M. Buongiorno Nardelli, and S. Curtarolo, *High-throughput computational screening of thermal conductivity, Debye temperature, and Grüneisen parameter using a quasiharmonic Debye model*, Phys. Rev. B **90**, 174107 (2014), doi:10.1103/PhysRevB.90.174107.
- [53] C. Toher, C. Oses, J. J. Plata, D. Hicks, F. Rose, O. Levy, M. de Jong, M. Asta, M. Fornari, M. Buongiorno Nardelli, and S. Curtarolo, *Combining the AFLOW GIBBS and elastic libraries to efficiently and robustly screen thermomechanical properties of solids*, Phys. Rev. Materials **1**, 015401 (2017), doi:10.1103/PhysRevMaterials.1.015401.
- [54] J.-P. Poirier, *Introduction to the Physics of the Earth's Interior* (Cambridge University Press, 2000), 2nd edn.
- [55] J. J. Plata, P. Nath, D. Usanmaz, J. Carrete, C. Toher, M. de Jong, M. D. Asta, M. Fornari, M. Buongiorno Nardelli, and S. Curtarolo, *An efficient and accurate framework for calculating lattice thermal conductivity of solids: AFLOW-AAPL Automatic Anharmonic Phonon Library*, npj Comput. Mater. **3**, 45 (2017), doi:10.1038/s41524-017-0046-7.
- [56] J. Sun, R. C. Remsing, Y. Zhang, Z. Sun, A. Ruzsinszky, H. Peng, Z. Yang, A. Paul, U. Waghmare, X. Wu, M. L. Klein, and J. P. Perdew, *Accurate first-principles structures and energies of diversely bonded systems from an efficient density functional*, Nat. Chem. **8**, 9 (2016), doi:10.1038/nchem.2535.
- [57] C. E. Calderon, J. J. Plata, C. Toher, C. Oses, O. Levy, M. Fornari, A. Natan, M. J. Mehl, G. L. W. Hart, M. Buongiorno Nardelli, and S. Curtarolo, *The AFLOW standard for high-throughput materials science calculations*, Comput. Mater. Sci. **108**, 233–238 (2015), doi:10.1016/j.commatsci.2015.07.019.
- [58] W. Kohn and L. J. Sham, *Self-Consistent Equations Including Exchange and Correlation Effects*, Phys. Rev. **140**, A1133 (1965), doi:10.1103/PhysRev.140.A1133.
- [59] U. von Barth and L. Hedin, *A local exchange-correlation potential for the spin polarized case: I*, J. Phys. C: Solid State Phys. **5**, 1629 (1972), doi:10.1088/0022-3719/5/13/012.
- [60] O. Levy, R. V. Chepulskii, G. L. W. Hart, and S. Curtarolo, *The New Face of Rhodium Alloys: Revealing Ordered Structures from First Principles*, J. Am. Chem. Soc. **132**, 833–837 (2010), doi:10.1021/ja908879y.
- [61] O. Levy, G. L. W. Hart, and S. Curtarolo, *Structure maps for hcp metals from first-principles calculations*, Phys. Rev. B **81**, 174106 (2010), doi:10.1103/PhysRevB.81.174106.
- [62] O. Levy, M. Jahnátek, R. V. Chepulskii, G. L. W. Hart, and S. Curtarolo, *Ordered Structures in Rhenium Binary Alloys from First-Principles Calculations*, J. Am. Chem. Soc. **133**, 158–163 (2011), doi:10.1021/ja1091672.
- [63] S. Curtarolo, W. Setyawan, G. L. W. Hart, M. Jahnátek, R. V. Chepulskii, R. H. Taylor, S. Wang, J. Xue, K. Yang, O. Levy, M. J. Mehl, H. T. Stokes, D. O. Demchenko, and D. Morgan, *AFLOW: An automatic framework for high-throughput materials discovery*, Comput. Mater. Sci. **58**, 218–226 (2012), doi:10.1016/j.commatsci.2012.02.005.
- [64] K. Yang, C. Oses, and S. Curtarolo, *Modeling Off-Stoichiometry Materials with a High-Throughput Ab-Initio Approach*, Chem. Mater. **28**, 6484–6492 (2016), doi:10.1021/acs.chemmater.6b01449.
- [65] A. R. Supka, T. E. Lyons, L. S. I. Liyanage, P. D'Amico, R. Al Rahal Al Orabi, S. Mahatara, P. Gopal, C. Toher, D. Ceresoli, A. Calzolari, S. Curtarolo, M. Buongiorno Nardelli, and M. Fornari, *AFLOW π : A minimalist approach to high-throughput ab initio calculations including the generation of tight-binding hamiltonians*, Comput. Mater. Sci. **136**, 76–84 (2017), doi:10.1016/j.commatsci.2017.03.055.
- [66] G. Kresse and J. Furthmüller, *Efficient iterative schemes for ab initio total-energy calculations using a plane-wave basis set*, Phys. Rev. B **54**, 11169–11186 (1996), doi:10.1103/PhysRevB.54.11169.
- [67] W. Sun, A. Holder, B. Orvañanos, E. Arca, A. Zakutayev, S. Lany, and G. Ceder, *Thermodynamic Routes to Novel Metastable Nitrogen-Rich Nitrides*, Chem. Mater. **29**, 6936–6946 (2017), doi:10.1021/acs.chemmater.7b02399.
- [68] W. Sun, C. J. Bartel, E. Arca, S. R. Bauers, B. Matthews, B. Orvañanos, B.-R. Chen, M. F. Toney, L. T. Schelhas, W. Tumas, J. Tate, A. Zakutayev, S. Lany, A. M. Holder, and G. Ceder, *A map of the inorganic ternary metal nitrides*, Nat. Mater. **18**, 732–739 (2019), doi:10.1038/s41563-019-0396-2.
- [69] P. Sarker, T. Harrington, C. Toher, C. Oses, M. Samiee, J.-P. Maria, D. W. Brenner, K. S. Vecchio, and S. Curtarolo, *High-entropy high-hardness metal carbides discovered by entropy descriptors*, Nat. Commun. **9**, 4980 (2018), doi:10.1038/s41467-018-07160-7.
- [70] M. R. Ranade, F. Tessier, A. Navrotsky, V. J. Leppert, S. H. Risbud, F. J. DiSalvo, and C. M. Balkas, *Enthalpy of Formation of Gallium Nitride*, J. Phys. Chem. B **104**, 4060–4063 (2000), doi:10.1021/jp993752s.
- [71] J. M. McHale, A. Navrotsky, G. R. Kowach, V. E. Balbarin, and F. J. DiSalvo, *Energetics of Ternary Nitrides: Li-Ca-Zn-N and Ca-Ta-N Systems*, Chem. Mater. **9**, 1538–1546 (1997), doi:10.1021/cm970244r.
- [72] J. M. McHale, A. Navrotsky, and F. J. DiSalvo, *Energetics of Ternary Nitride Formation in the (Li,Ca)-(B,Al)-N System*, Chem. Mater. **11**, 1148–1152 (1999), doi:10.1021/cm981096n.
- [73] M. J. Mehl, D. Hicks, C. Toher, O. Levy, R. M. Hanson, G. L. W. Hart, and S. Curtarolo, *The AFLOW Library of Crystallographic Prototypes: Part 1*, Comput. Mater. Sci. **136**, S1–S828 (2017), doi:10.1016/j.commatsci.2017.01.017.
- [74] D. Hicks, M. J. Mehl, E. Gossett, C. Toher, O. Levy, R. M. Hanson, G. L. W. Hart, and S. Curtarolo, *The AFLOW Library of Crystallographic Prototypes: Part 2*, Comput. Mater. Sci. **161**, S1–S1011 (2019), doi:10.1016/j.commatsci.2018.10.043.
- [75] D. Hicks, M. J. Mehl, M. Esters, C. Oses, O. Levy, G. L. W. Hart, C. Toher, and S. Curtarolo, *The AFLOW Library of Crystallographic Prototypes: Part 3*, Comput. Mater. Sci. **199**, 110450 (2021), doi:10.1016/j.commatsci.2021.110450.

[76] D. Hicks, C. Oses, E. Gossett, G. Gomez, R. H. Taylor, C. Toher, M. J. Mehl, O. Levy, and S. Curtarolo, *AFLOW-SYM: platform for the complete, au-*

tomatic and self-consistent symmetry analysis of crystals, Acta Crystallogr. Sect. A **74**, 184–203 (2018), doi: 10.1107/S2053273318003066.